Macromolecules **2008**, *41*, 9556–9564

Low Dielectric Constant and High Organosolubility of Novel Polyimide Derived from Unsymmetric 1,4-Bis(4-aminophenoxy)-2,6-di-*tert*-butylbenzene

Yaw-Terng Chern* and Jeng-Yu Tsai

Department of Chemical Engineering, National Taiwan University of Science and Technology, Taipei, Taiwan, Republic of China

Received October 14, 2008; Revised Manuscript Received November 5, 2008

ABSTRACT: A series of new polyimides (PIs) containing *tert*-butyl side groups were synthesized via a polycondensation of 1,4-bis(4-aminophenoxy)-2,6-di-*tert*-butylbenzene (**4**) with various aromatic tetracarboxylic dianhydrides. The introduction of the asymmetric di-*tert*-butyl groups is an effective way to increase the interchain distance and decrease in the intermolecular force and packing ability of the resulting polymers. Thus, this novel PIs exhibit a low dielectric constant (2.74−2.92), low moisture absorption (0.32−1.53%), excellent solubility, and high glass transition temperature (276−398 °C). The PIs derived from the very rigid pyromellitic dianhydride (PMDA) were soluble in *N*-methyl-2-pyrrolidone, *N,N*-dimethylacetamide, chloroform, tetrahydrofuran, and cyclohexanone. The crystal structure of 1,4-bis(4-phthalimidophenoxy)-2,5-di-*tert*-butylbenzene indicates that the symmetric compound leads to the strong intermolecular interaction and good packing ability. In the ^{1}H spectrum of the diamine **4**, the protons of 4-aminophenoxy moiety are not chemical shift equivalent. This is because the steric hindrance of the bulky di-*tert*-butyl groups prevents the benzene ring of 4-aminophenoxy moiety from rotating freely. In addition, the effect of symmetric and asymmetric di-*tert*-butyl pendent groups on the properties of PIs was discussed.

Introduction

Because of rapid advancement in the microelectronic industry, the enhanced performance of tightly packed circuitry has become an increasingly relevant issue. Therefore, various approaches have been conducted to decrease the dielectric constant while maintaining thermal and mechanical properties of the interlayer dielectric materials. Fluorine-containing polymers with low dielectric constants have been reported.[1−3] For example, the highly fluorinated polyimides have dielectric constants of ∼2.5.[1,2] Fluorinated polyaryl ethers based on decafluorobiphenyl exhibit a thermal stability comparable to that polyimides, ∼10−40 times lower moisture absorption, dielectric constants in the mid-twos, and good retention of the storage modulus above the glass transition temperatures.[3] Recently, Swager et al. reported a new low k material using the ring-opening olefin metathesis polymerization of a polymer with triptycene unit.[4] Tsuchiya also reported a new low k material by oxidative coupling polymerization of a polymer with naphthylene unit.[5] In addition, an alternative to push dielectric constants even lower are the closed-cell organic and/or inorganic polymeric foams, i.e., materials with significant void volumes.[6] Very recently, Kakimoto et al. also reported a new low k of PIs containing POSS in main chain.[7]

Aromatic polyimides (PIs) are an important class of thermally stable polymers because of their excellent thermal stability, good chemical resistance, mechanical strength, and low dielectric constants.[8] They have been widely used in microelectronic, aviation, liquid crystal display, and separation industries. However, aromatic PIs are difficult to process because they are insoluble in most organic solvents and do not flow below their decomposition temperatures, thus restricting their applications. The increasing demands of this application have stimulated extensive research on soluble PIs that can exhibit certain advantageous properties. Typical approaches include the introduction of flexible or kinked linkages,[9,10] bulky substituents,[11−13] noncoplanar structures,[14−16] and spiro-skeletons[17,18] into the polymer backbone.

Recently, one attractive method for improved processability has been to incorporate geometrically asymmetric diamine[19−22] or dianhydride[23−25] components into the PI main chain. These structural modifications have led to new PIs with improved solubility and melt processability and other desirable properties. So far, however, most studies have focused on the effect of asymmetric structures on the solubility. There is no report about the effect of asymmetric structures on their electric property such as dielectric constant. Incorporation of bulky pendent groups can impart a significant increase in T_g by restricting segmental mobility, while providing good solubility due to decreased packing and crystallinity.[11] However, PIs derived from the *tert*-butyl-substituted diamines showed a limited solubility. For example, Yang studied a series of PIs derived from 1,4-bis(4-aminophenoxy)-2-*tert*-butylbenzene.[20] These materials derived from PMDA, 4,4′-carbonyldiphthalic anhydride (BTDA), and 3,3′,4,4′-biphenyltetracarboxylic anhydride (BPDA) were not soluble in the tested solvents. PIs derived from the symmetry-substituted diamines gave deteriorated solubility. For example, Liaw reported that almost all of the PIs derived from symmetric 1,4-bis(4-aminophenoxy)-2,5-di-*tert*-butylbenzene were insoluble in the tested solvent.[22]

Herein, we synthesized new PIs derived from 1,4-bis(4-aminophenoxy)-2,6-di-*tert*-butylbenzene with aromatic dianhydrides. Because the new diamine monomer is molecularly asymmetric, the resulting PIs should exhibit excellent solubility and retain other desirable properties such as low dielectric constant. This work was also performed to obtain fundamental information on symmetric and asymmetric substituents/property relationships.

Experimental Section

Materials. Pyromellitic dianhydride (PMDA), 3,3′,4,4′-benzophenonetetracarboxylic dianhydride (BTDA), 4,4′-oxydiphthalic anhydride (ODPA), 4,4′-hexafluoroisopropylidene diphthalic anhydride (6FDA), 3,3′,4,4′-biphenyltetracarboxylic anhydride (BPDA),

* Corresponding author: Tel +886-27376646; Fax +886-27376644; e-mail ytchern@mail.ntust.edu.tw.

10.1021/ma802305q CCC: $40.75
Published on Web 11/21/2008

and naphthalene-1,4,5,8-tetracarboxylic dianhydride (NTDA) were sublimated prior to use. *m*-Cresol was purified by distillation under reduced pressure over calcium hydride and stored over 4 Å molecular sieves. According to a previous method, 1,4-bis(4-aminophenoxy)-2,5-di-*tert*-butylbenzene was synthesized from hydroquinone.[19]

Instrumentation. A Bio-Rad FTS-40 FTIR spectrophotometer was used to record IR spectra (KBr pellets). In a typical experiment, an average of 20 scans per sample was made. MS spectra were obtained by using a JEOL JMS-D300 mass spectrometer. ^{1}H and ^{13}C NMR spectra were recorded on Bruker AV 500 Fourier transform nuclear magnetic resonance spectrometers using tetramethylsilane (TMS) as the internal standard. A PerkinElmer 240C elemental analyzer was used for elemental analysis. The X-ray crystallographic data were collected on a CAD-4 diffractometer. The analyses were carried out on a DEC station 3500 computer using NRCC SDP software. The melting points were obtained by a standard capillary milting point apparatus. Inherent viscosities of all polymers were determined at 0.5 g/dL using an Ubbelohde viscometer. Gel permeation chromatography (GPC) on soluble polymers was performed on an Applied Bio system at 70 °C with two PLgel 5 μm mixed-C columns in the NMP/LiBr (0.06 mol/L) solvent system. The flow rate was 0.5 mL/min, detection was by UV, and calibration was based on polystyrene standards. Qualitative solubility was determined using 0.1 g of polymer in 2.0 mL of solvent. A TA Instruments DSC 2010 differential scanning calorimeter and a PerkinElmer Diamond SII thermogravimetric analyzer were employed to study the transition data and thermal decomposition temperature of all the polymers. The differential scanning calorimeter (DSC) was run under a nitrogen stream at a flow rate 30 cm^3/min and a heating rate of 20 °C/min. The thermogravimetric analysis (TG) was determined under a nitrogen flow of 50 cm^3/min. Dynamic mechanical analysis (DMA) was performed on a TA Instruments DMA 2980 thermal analyzer system. A sample 10 mm in length, 2 mm in width, and ~0.06 mm in the thickness was used. The dynamic tensile mode was measured at 1 Hz frequency.

Tensile properties were determined from stress−strain curves with a Toyo Baldwin Instron UTM-III-500 with a load cell of 10 kg at a drawing speed of 5 cm/min. Measurements were performed at 28 °C with film specimens (about 0.1 mm thick, 1.0 cm wide, and 5 cm long), and an average of at least five individual determinations was used. Moisture absorption measurements were made with an ultramicrobalance of Sartorius model S3D-P on thin films (~40 μm). Measurements were taken immersing films of these polyimides in distilled water at 25 °C for 100 h. Dielectric constants were measured by the sputter-coated sensor using a dielectric analyzer (TA Instruments DEA 2970) on thin films. Gold electrodes were vacuum-deposited on both surfaced of dried films, followed by measuring at 25 °C in a sealed chamber at 0% relative humidity.

3,5-Di-*tert*-butyl-4-(4-nitrophenoxy)anisole (1). A flask was charged with 2,6-di-*tert*-butyl-4-methoxyphenol (10.0 g, 42.3 mmol), potassium carbonate (6.10 g, 44.2 mmol), 1-fluoro-4-nitrobenzene (6.20 g, 43.9 mmol), and dry dimethyl sulfoxide (DMSO, 54.0 mL). The reaction mixture was heated at 110 °C for 22 h with stirring under N_2. Then the reaction mixture was allowed to cool to room temperature and poured into distilled water. The yellow precipitate was collected by filtration. The product was washed with water and dried. The crude product was recrystallized from pentanol to afford 11.2 g (74.2%) of yellow crystals; mp 88−90 °C. IR (KBr): 1356, 1530, and 2970 cm^{-1}. ^{1}H (CDCl$_3$) δ: 1.24 (s, 18H, −C(CH$_3$)$_3$), 3.86 (s, 3H, CH$_3$), 6.19 (d, J = 9.00 Hz, 1H, H-1), 6.94 (s, 2H, H-5), 7.18 (d, J = 11.50 Hz, 1H, H-4), 8.04 (d, J = 9.00 Hz, 1H, H-2), and 8.29(d, J = 11.50 Hz, 1H, H-3) ppm. ^{13}C NMR (CDCl$_3$) δ: 32.31 (−C(*C*H$_3$)$_3$), 36.57 (−*C*(CH$_3$)$_3$), 56.02 (OCH$_3$), 112.91 (C-5), 115.14 (C-1), 117.84 (C-4), 126.25 (C-2), 126.90 (C-3), 142.29 (C-6), 144.96 (C-9), 145.29 (C-8), 156.92 (C-10), and 167.32 ppm (C-7). Anal. Calcd for $C_{21}H_{27}NO_4$: C, 70.59; H, 7.56; N, 3.92. Found: C, 70.31; H, 7.61; N, 3.88.

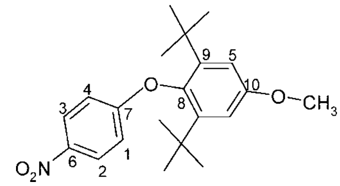

3,5-Di-*tert*-butyl-4-(4-nitrophenoxy)phenol (2). A mixture of 6.00 g (16.8 mmol) of **1** and 48.0 g of pyridine hydrochloride was heated at 160 °C for 20 h under nitrogen. The reaction mixture was then poured into distilled water. Then the precipitate was collected by filtration, and then the crude product was washed with water and dried. The product was recrystallized from methanol to afford 3.74 g (64.9%) of gray crystals; mp 193−195 °C. IR (KBr): 1355, 1542, 2970, and 3420 cm^{-1}. ^{1}H (DMSO-d_6) δ: 1.13 (s, 18H, CH$_3$), 6.20 (d, J = 11.56 Hz, 1H, H-1), 6.81 (s, 2H, H-5), 7.27 (d, J = 11.58 Hz, 1H, H-4), 8.10 (d, J = 11.58 Hz, 1H, H-2), 8.26 (d, J = 11.55 Hz, 1H, H-3), and 9.32 ppm (s, 1H, OH). ^{13}C NMR (DMSO-d_6) δ: 32.05 (CH$_3$), 35.83 (−*C*(CH$_3$)$_3$), 114.27 (C-5), 115.32 (C-1), 117.98 (C-4), 126.49 (C-2), 126.87 (C-3), 141.86 (C-6), 143.46 (C-8), 144.09 (C-9), 155.04 (C-10), and 167.13 (C-7) ppm. Anal. Calcd for $C_{20}H_{25}NO_4$: C, 69.97; H, 7.27; N, 4.08. Found: C, 69.78; H, 7.31; N, 3.97.

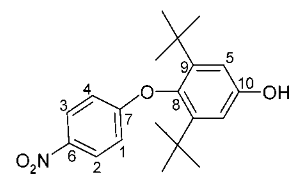

1,4-Bis(4-nitrophenoxy)-2,6-di-*tert*-butylbenzene (3). A mixture of 3.50 g (10.2 mmol) compound **2**, 2.10 g (14.8 mmol) of 1-fluoro-4-nitrobenzene, 2.10 g (15.2 mmol) of potassium carbonate, and 18 mL of dry *N,N*-dimethylformamide (DMF) was refluxed for 14 h under nitrogen. The reaction mixture was poured into distilled water. The precipitate was collected by filtration and recrystallized from pentanol to afford 4.02 g (84.9%) of pale-yellow crystals; mp 133−135 °C. IR (KBr): 1356, 1565, 2972, and 3060 cm^{-1}. ^{1}H (DMSO-d_6) δ: 1.18 (s, 18H, CH$_3$), 6.31 (d, J = 11.88 Hz, 1H, H-1), 7.21 (s, 2H, H-5), 7.36 (d, J = 8.96 Hz, 2H, H-6), 7.41 (d, J = 11.56 Hz, 1H, H-4), 8.16 (d, J = 11.85 Hz, 1H, H-2), and 8.31 ppm (m, 3H, H = 3, 7). ^{13}C NMR (DMSO-d_6) δ: 31.89 (CH$_3$), 36.34 (−*C*(CH$_3$)$_3$), 115.34 (C-1), 117.84 (C-5), 118.33 (C-4), 120.44 (C-6), 126.67 (C-2), 126.93 (C-3), 127.04 (C-7), 142.29 (C-14), 142.89 (C-8), 144.43 (C-10), 146.04 (C-11), 161.17 (C-12), 163.65 (C-13), and 166.34 ppm (C-9). Anal. Calcd for $C_{26}H_{28}N_2O_6$: C, 67.24; H, 6.03; N, 6.05. Found: C, 67.11; H, 6.09; N, 6.01.

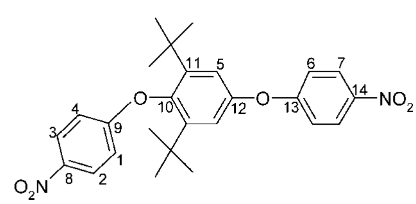

1,4-Bis(4-aminophenoxy)-2,6-di-*tert*-butylbenzene (4). A flask was charged with **3** (7.00 g, 15.1 mmol), 35.0 mL of hydrazine monohydrate, 50.0 mL of ethanol, and 0.140 g of 10% palladium on carbon (Pd−C). The mixture was heated to reflux for 2 days. The mixture was then filtered to remove the Pd−C, and the reaction mixture was poured into distilled water. The precipitate was collected by filtration, and the crude solid was recrystallized from pentanol to yield 4.45 g (72.9%) of white crystals; mp 158−160 °C. IR (KBr): 2970, 3220, 3350, and 3450 cm^{-1}. ^{1}H (DMSO-d_6) δ: 1.15 (s, 18H, CH$_3$), 4.59 (s, 2H, NH$_2$), 4.93 (s, 2H, NH$_2$), 5.72 (brs, 1H, H-1), 6.37 (brs, 1H, H-2), 6.61 (brd, J = 8.50 Hz, 3H, H-3,7), 6.80 (brd, J = 8.68 Hz, 3H, H-4,6), and 6.86 (s, 2H, H - 5) ppm. ^{13}C NMR (DMSO-d_6) δ: 32.01 (CH_3), 36.14 ($-C(CH_3)_3$), 114.78 (C-1), 114.91 (C-2), 115.19 (C-5), 115.66 (C-7), 116.37 (C-3), 117.16 (C-4), 121.30 (C-6), 143.03 (C-8), 145.29 (C-11), 145.78 (C-14), 146.63 (C-10), 147.14 (C-9), 153.15 (C-12), and 155.26 ppm (C-13). Anal. Calcd for $C_{26}H_{32}N_2O_2$: C, 77.23; H, 7.92; N, 6.33. Found: C, 77.05; H, 7.97; N, 6.28. Crystal data: $C_{26}H_{32}N_2O_2$, colorless crystal, 0.32 × 0.25 × 0.20 mm, monoclinic with a = 8.789 (10) Å, b = 22.999 (4) Å, c = 12.117 (3) Å, α = 90°, β = 107.3370 (6)°, γ = 90° with D_c = 1.150 mg/m^3 for Z = 4, V = 2337.52 (8) Å^3, T = 295 K, λ = 0.710 73 Å, F(000) = 872, final R indices: R1 = 0.0639, WR2 = 0.1749.

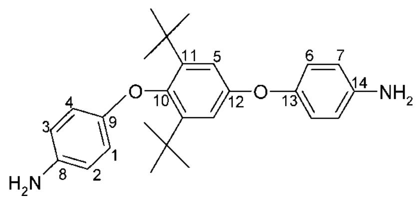

Representative Procedure for the Preparation of Polyimides (5). Polymerization was carried out in a one-step chemical imidization. The diamine **4** (0.897 g, 2.22 mmol), PMDA (0.485 g, 2.22 mmol), and m-cresol (10.0 mL) were added to a three-necked flask equipped with a stirrer, a nitrogen inlet, and a distillation head. Isoquinoline (6 drops) was added to the flask. After the mixture was stirred at room temperature for 3 h and heated at 80 °C for 2 h, it was heated to 200−210 °C for 14 h. Water was continuously distilled from the reaction mixture. The solution was poured into a methanol (500 mL). The polymer that precipitated was collected, filtered, washed with ethanol and water, and dried under reduced pressure at 200 °C for 8 h. The yields of polyimides were 92%. The inherent viscosity of **5a** was 0.56 dL/g, as measured at a concentration of 0.5 g/dL in NMP at 30 °C. IR (KBr): 2970, 1781, 1720, and 1383 cm^{-1}. ^{1}H (DMSO-d_6) δ: 1.24 (18H, CH_3), 6.26 (1H, H-1), 7.16 (2H, H- 5), 7.30 (3H, H-4,6), 7.50 (4H, H-2,3,7), and 8.33 ppm (2H, H-8).

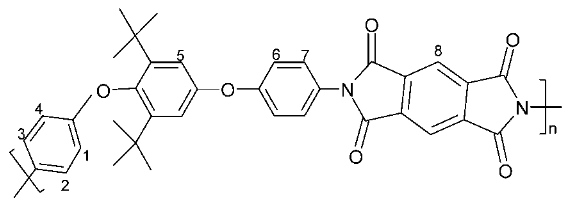

1,4-Bis(4-phthalimidophenoxy)-2,6-di-*tert*-butylbenzene (7). The diamine **4** (0.804 g, 1.99 mmol), phthalic anhydride (0.591 g, 3.98 mmol), and m-cresol (10 mL) were added to a three-necked flask equipped with a stirrer and a nitrogen inlet. Isoquinoline (6 drops) was added to the flask. After the mixture was stirred at room temperature for 3 h, it was heated to 200−210 °C for 14 h. The solution was poured into a hot water (500 mL). The product that precipitated was collected, filtered, washed with ethanol and water, and dried under reduced pressure at 200 °C for 8 h. The yield of **6** was 92%. IR (KBr): 2970, 1780, 1722, and 1380 cm^{-1}. Crystal data: $C_{42}H_{36}N_2O_6$, colorless crystal, 0.55 × 0.08 × 0.03 mm, monoclinic with a = 19.9081 (2) Å, b = 6.1276 (1) Å, c = 28.4745 (4) Å, α = 90°, β = 93.3711 (6)°, γ = 90° with D_c = 1.273 mg/m^3 for Z = 4, V = 3467.56 (8) Å^3, T = 295 K, λ = 0.710 73 Å, F(000) = 1400, final R indices: R1 = 0.0597, WR2 = 0.1343.

1,4-Bis(4-phthalimidophenoxy)-2,5-di-*tert*-butylbenzene (8). Compound **8** was synthesized from 1,4-bis(4-aminophenoxy)-2,5-di-*tert*-butylbenzene using the same procedure used for compound **7**: The yield of was 94%. IR (KBr): 2974, 1780, 1721, and 1382 cm^{-1}. Crystal data: $C_{42}H_{36}N_2O_6$, colorless crystal, 0.25 × 0.20 × 0.10 mm, triclinic with a = 5.9312 (1) Å, b = 8.4961 (1) Å, c = 17.4280 (2) Å, α = 77.6428 (7)°, β = 82.0612 (6)°, γ = 83.4427 (6)° with D_c = 1.304 mg/m^3 for Z = 1, V = 846.41 (2) Å^3, T = 295 K, λ = 0.710 73 Å, F(000) = 350, final R indices: R1 = 0.0471, WR2 = 0.1138.

Scheme 1

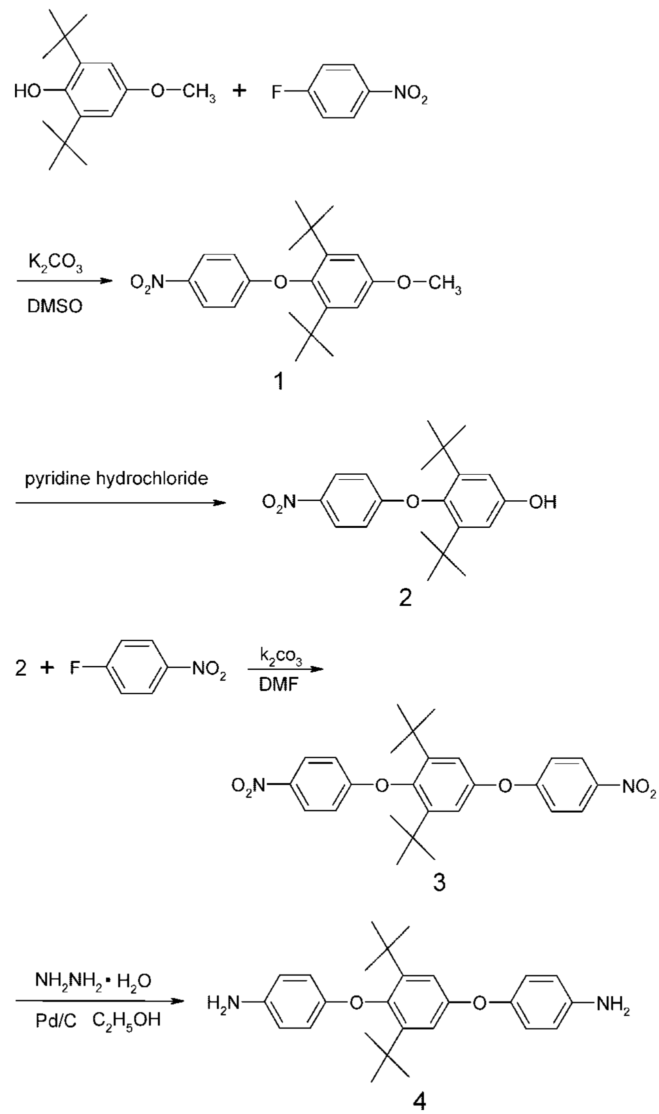

Results and Discussion

Monomer Synthesis. Four steps were employed to synthesize the new diamine **4** from 2,6-di-*tert*-butyl-4-methoxyphenol as shown in Scheme 1. An aromatic nucleophilic substitution (S_NAr) reaction of 2,6-di-*tert*-butyl-4-methoxyphenol with 1-fluoro-4-nitrobenzene in DMSO in the presence of potassium carbonate as an acid acceptor generated the nitro compound **1**, which was left off the methyl groups in the presence of pyridine hydrochloride to produce compound **2**. A S_NAr reaction of **2** with 1-fluoro-4-nitrobenzene in DMF in the presence of potassium carbonate as an acid acceptor generated the dinitro compound **3**, which was hydrogenated to generate the new diamine **4**. Elemental analysis, IR, and NMR spectroscopic techniques were used to identify structures of the intermediate compounds (**1**, **2**, and **3**) and the target diamine monomer (**4**). The ^{1}H spectra of the monomers (**3** and **4**) are shown in Figure 1. Interestingly, in the ^{1}H spectrum of compound **3**, H-1 and H-4 are not magnetically equivalent, and H-2 and H-3 are not magnetically equivalent. This is because the steric hindrance of the bulky di-*tert*-butyl groups prevents the benzene ring of the neighboring 4-aminophenoxy moiety from rotating freely. Moreover, H-1 appeared farthest upfield at 6.31 ppm (Figure

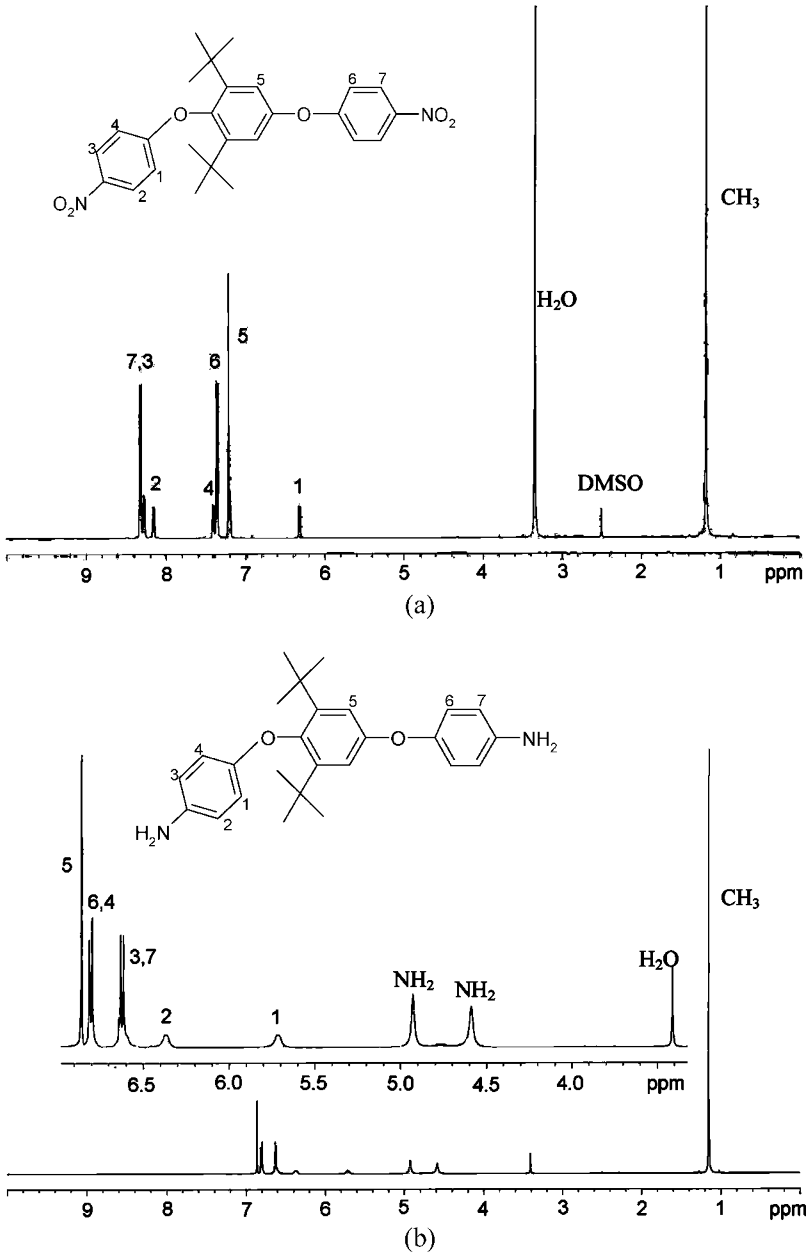

Figure 1. ^{1}H (500 MHz) spectra of (a) **3** and (b) **4**.

1a) due to the ring current effect caused by neighboring benzene. Compound **4** showed the same behavior, and H-1 appeared farthest upfield at 5.72 ppm (Figure 1b). Interestingly, H-1 to H-4 produced the individual broad singlet signals (Figure 1b). The signals appearing at 4.59 and 4.93 ppm are peculiar to the amino groups (Figure 1b). Elemental analysis data, the NMR spectra, and the IR spectra confirmed all monomers reported herein. In addition, X-ray diffraction analysis confirmed the structure of **4** (in Figure 2). X-ray crystal data for **4** were acquired from a single crystal, as obtained by slowly crystallizing from pentanol solution. In X-ray structure of **4**, the dihedral angles between the central and outer rings are 85° and 68° for C(21)−C(22) and C(15)−C(16), respectively (in Figure 2). The structure of **4** exhibited asymmetrical and bulky molecular characteristics.

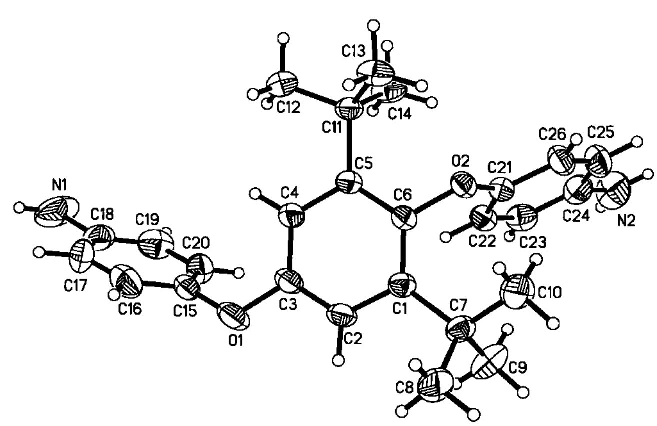

Figure 2. X-ray structure of **4**.

Conformations of Compounds 7 and 8. Single crystals of compounds **7** and **8** suitable for X-ray analysis were grown by slow evaporation of solution in the individual NMP solutions. Figure 3 show various views of the crystal structures and packing of compound **7**. Compound **7** adopts a much more generally extended conformation. This geometry is achieved by a combination of (i) a relationship between rings A and B which

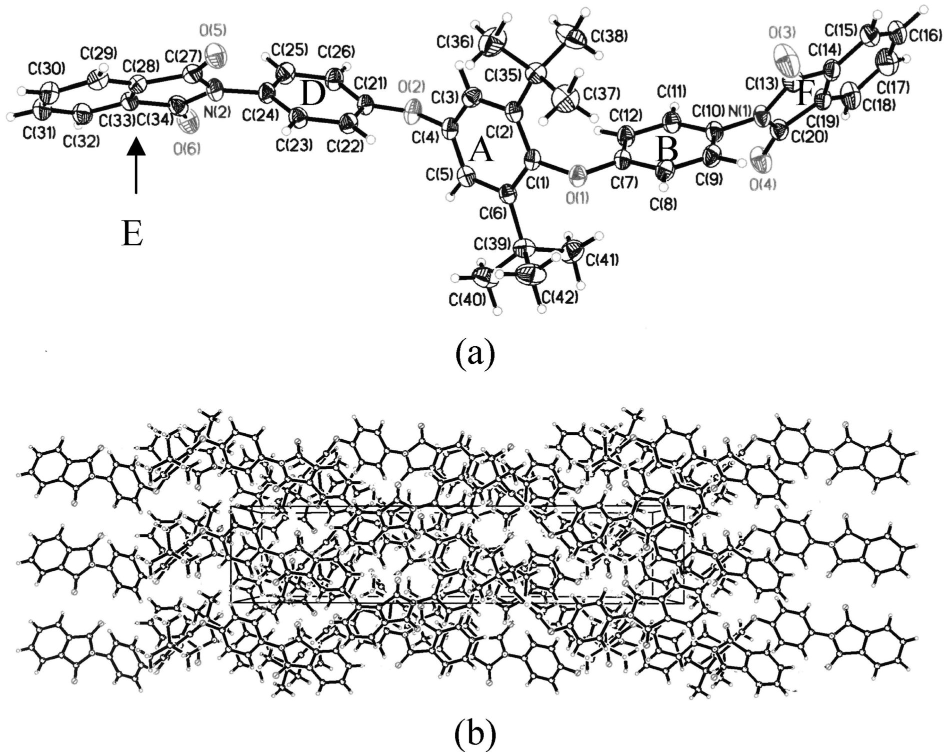

Figure 3. (a) ORTEP diagram and (b) crystal packing view along the *a*-axis of compound **7**.

is nearer orthogonal (inter-ring torsion angle 84°, 119° bond angle at oxygen), (ii) a similar relationship between rings A and D which is near orthogonal (inter-ring torsion angle 85°, 119° bond angle at oxygen), (iii) an inter-ring torsion angle between the imide unit F and the ring B of 77°, and (iv) an inter-ring torsion angle between the imide unit E and the ring D of 51°. Figure 3b shows that the crystal packing of compound **7** is confused and disorderly. Figure 4 show various view of the crystal structures and packing of compound **8**. The structure of **8** exhibited symmetrical molecular characteristics. This geometry is achieved by a combination of (i) a relationship between rings A and B which is nearer orthogonal (inter-ring torsion angle 75°, 118° bond angle at oxygen) and (ii) an inter-ring angle between the imide unit D and the ring B of 53°. Figure 4b shows that the oxygen of pyromellitimide unit interacts particularly with the hydrogen of the benzene on the neighboring chain (O3···H15C; O3B···H15A; O2···H12E; O2C···H12A). The distance from the O3B to H15A is 2.49 Å, and the distance from the O2 to H12E is 2.54 Å. Figure 4c shows that the crystal packing of compound **8** is relatively orderly. Because of the symmetrical structure of compound **8**, **8** had slightly bigger density than **7** (see Experimental Section). Because of the bulky *tert*-butyl groups, both **7** and **8** had the noncoplanar structures. Comparing compounds **7** and **8**, it is evident that the symmetrical compound (i.e., **8**) leads to the strong intermolecular interaction and good packing ability. In general, bond lengths and bond angles vary only very slightly between closely related molecular systems, so reliable data of this type can be obtained from single crystal analyses of small molecules related to the polymer in question. Thus, the crystal structures of small molecules (i.e., **7** and **8**) suggest that the conformations of **5** and **6** series exhibited the bulky and noncoplanar molecular characteristics.

Synthesis of Polyimides. The polyimides were prepared by the one-step method in *m*-cresol at 200−210 °C (Scheme 2). The formation of PIs was confirmed by IR and ^{1}H spectroscopy (see Experimental Section). The inherent viscosities and GPC molecular weights of PIs are shown in Table 1 The soluble PIs **5** series had high inherent viscosities of 0.42−1.13 dL/g. Table 1 also indicates that the M_n's of **5** series are 25 000−50 000. The flexible and toughness of PI films **5** series were obtained by casting from their NMP solution onto a glass plate and drying at 200 °C for 5 h under vacuum.

Characterization of Polymers. These PIs solubilities were tested in various solvents. It is well-known that aromatic PIs generally show rather poor solubility in organic solvents, especially for those derived from rigid dianhydrides such as PMDA and NTDA. Table 2 summarizes those results. The PIs **5** series show excellent solubility in the tested solvents. All **5** series except **5f** were soluble in NMP, DMAc, chloroform, *o*-chlorophenol, THF, and cyclohexanone. It is surprising that PI **5a**, which was prepared from the rigid PMDA, were soluble in NMP, DMAc, chloroform, THF, *o*-chlorophenol, and cyclohexanone. Even PI **5f** derived from the very rigid NTDA was soluble in NMP, *o*-chlorophenol, and chloroform. The **5** series containing asymmetric *tert*-butyl pendent groups revealed an significantly enhanced solubility in comparison with that of the corresponding analogues of the PIs derived from symmetric 1,4-bis(4-aminophenoxy)-2,5-di-*tert*-butylbenzene. The crystal structures of small molecules (i.e., **7** and **8**) suggest that the conformations of **5** and **6** series exhibited the bulky and noncoplanar molecular characteristics. However, the **6** series exhibited poor solubility. The increased solubility of **5** series is ascribed to the fact that the introduction of the asymmetric *tert*-butyl groups leads to the formation of configuration isomers of the repeat unit along the polymer backbone and causes the decrease in the intermolecular force and packing ability of the resulting polymers.

Table 3 summarizes the dielectric constants, moisture absorptions, and mechanical properties of the films. The mechanical properties were determined via an Instron machine. The mechanical properties of **5** series, in general, are satisfactory. All PIs **5** series had high tensile strength of 87−124 MPa, and they also gave fairly high values of elongation to break. Although the introduction of asymmetric *tert*-butyl units in **5** series leading to reducing intermolecular force between the

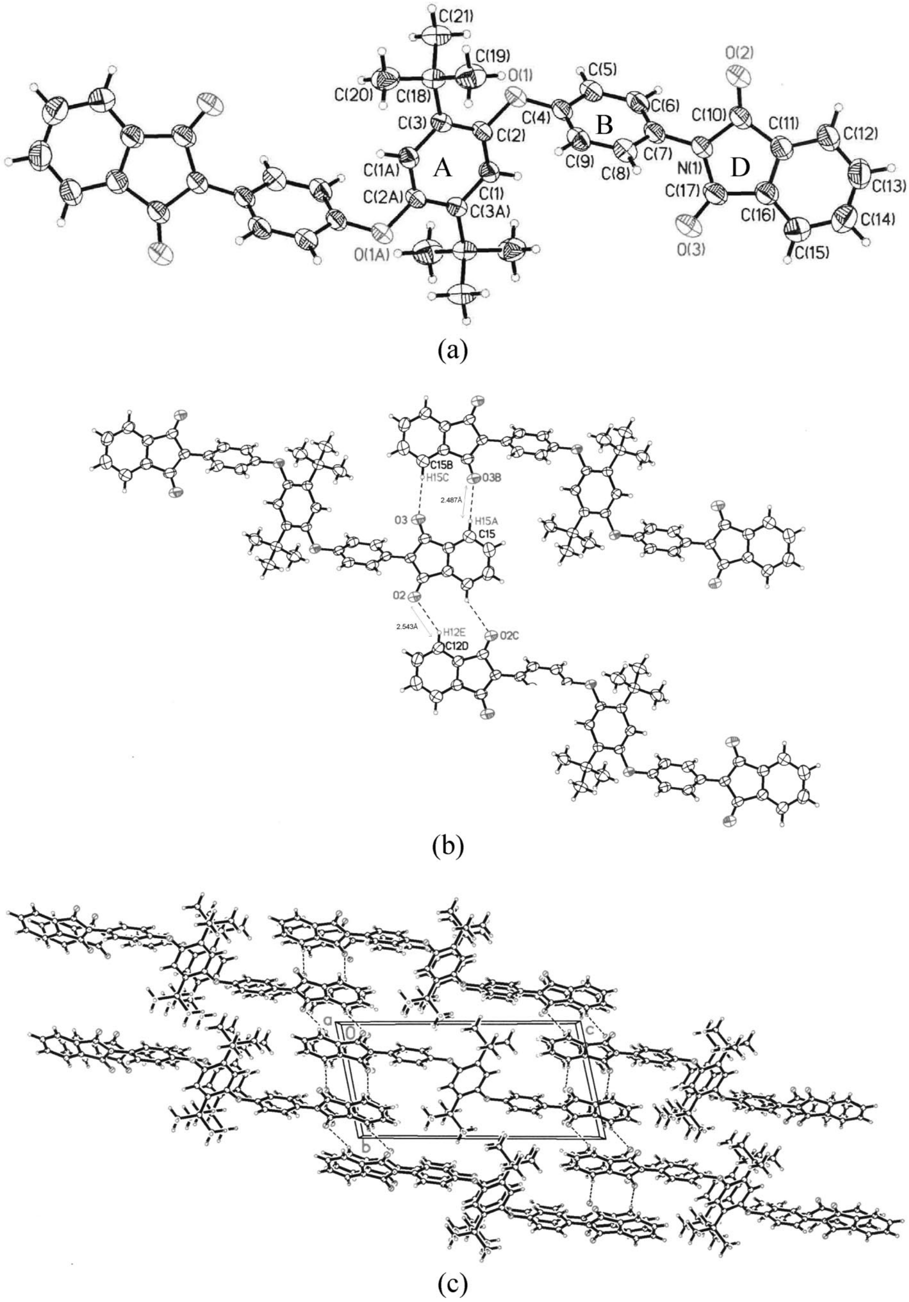

Figure 4. (a) ORTEP diagram, (b) one trimeric pair, and (c) crystal packing view along the *a*-axis of compound **8**.

polymer chains, they had even high tensile strength. Polymers **5** series also had low moisture absorption of 0.32−1.53%. The low moisture absorption is attributed to the fact that the **5** series contained the water proofing effect of the *tert*-butyl groups. Because of the water proofing effect of the trifluoromethyl groups, **5d** had significantly lower moisture absorption than the other **5** series. The **5** series containing the *tert*-butyl groups in the main chain also exhibited low dielectric constants in the range of 2.74−2.92, which is significantly lower than that (3.30) of PI film prepared from PMDA and 4,4′-oxidianiline (ODA). The low dielectric constant of **5** series is attributed to the fact that the introduction of the asymmetric bulky *tert*-butyl units loosened the polymer packing, subsequently leading to reducing their density. The **5** series with asymmetric *tert*-butyl pendent groups revealed a decreased dielectric constant in comparison with that of the corresponding analogues of the PIs **6** series with symmetric *tert*-butyl pendent groups. The low dielectric constant is attributed to the fact that the introduction of the asymmetric *tert*-butyl groups leads to the formation of configuration isomers of the repeat unit along the polymer backbone and causes the decrease in the intermolecular force and packing ability of the resulting polymers. These results suggest that the PIs containing the asymmetric pendent groups loosen the polymer packing, subsequently leading to reducing dielectric constant.

Thermal analysis was performed according to DSC, DMA, and TGA. The thermal properties of **5** series are listed in Table 4. Dynamic thermogravimetry showed the relatively good thermal stability of **5** series. Typical TGA curves of representative **5e** in both air and nitrogen atmospheres are shown in Figure 5. All **5** series exhibited good thermal stability with insignificant weight loss up to 400 °C. Their 10% weight-loss temperatures in nitrogen and air were recorded at 477−490 and 484−493 °C, respectively. The temperatures at weight loss of 10% of **5** series compare with those of the other PIs containing *tert*-butyl groups.[20] In DSC measurements, all **5** series showed distinct baseline shifts on their DSC heating traces, glass transition temperatures (T_g), defined as the temperature at the midpoint

Scheme 2

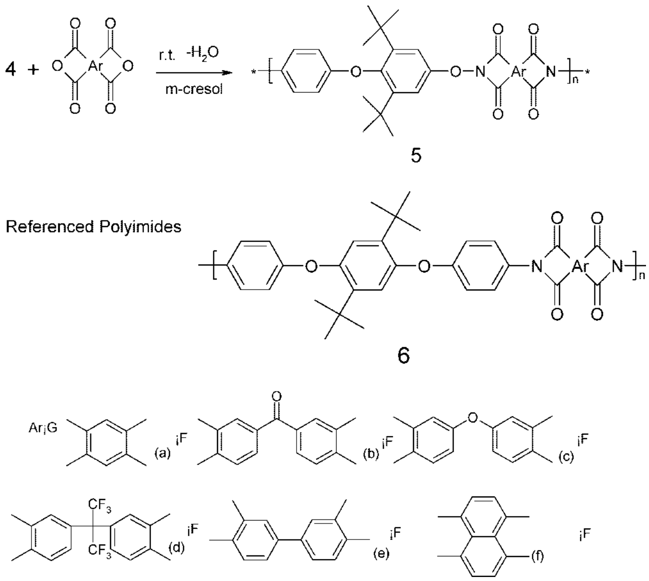

Table 1. Inherent Viscosities and GPC Molecular Weights of Soluble Polyimides

polymer	η_{inh}[a]	M_n[b] $\times 10^{-4}$	M_w/M_n
5a	0.56	3.1	2.4
5b	1.13	5.0	2.3
5c	0.59	3.6	2.2
5d	0.42	2.5	2.3
5e	0.85	4.1	2.1
5f	0.72[c]		
6c	(0.89)[d]		
6e	(1.22)[d]		

[a] Measured in NMP on 0.5 g/dL at 30 °C. [b] By GPC (relative to polystyrene). [c] Measured in *o*-chlorophenol on 0.5 g/dL at 30 °C. [d] Inherent viscosity of poly(amic acid).

Table 3. Physical Properties of Polyimides Films

polymer	strength to break (MPa)	elongation to break (%)	% H_2O absorption[a]	dielectric constant (dry, 1 kHz)
5a	87	5.9	1.26	2.86
5b	99	2.6	1.53	2.92
5c	124	9.1	1.14	2.88
5d	100	5.6	0.32	2.74
5e	111	8.1	1.03	2.85
5f	101	5.6	1.28	2.91
6c	106	5.0	1.10	3.02
6e	105	5.4	1.01	3.05
ref 1[b]	135	17.6	2.56	3.30

[a] Moisture absorption of polyimide films were measured immersing films of these polyimides in distilled water at 25 °C for 100 h. [b] A poly(ether imide) was synthesized from 4,4′-oxydianiline (ODA) and pyromellitic dianhydride (PMDA) in our laboratory. The inherent viscosity of its poly(amic acid) precursor was 1.25 dL/g.

Table 4. Thermal Properties of Polyimides

polymer	T_g (°C)		T_d (°C)[c]		char yield[d] (%)
	DSC[a]	DMA[b]	in air	in N_2	
5a	355	375	484	484	37
5b	289	312	487	477	38
5c	276	298	493	484	35
5d	285	310	487	482	39
5e	301	329	492	490	36
5f	375	398	488	486	42
6c	260	286	484	484	38
6e	290	315	494	491	35

[a] Temperature at which the middle of change of the heat capacity occurred from the second DSC heating scan at heating rate of 20 °C/min. [b] Temperature at which the peak maximum of tan δ occurred as recorded by DMA at a heating 5 °C/min. [c] Temperature at which 10% weight loss recorded by thermogravimetry at a heating rate of 10 °C/min. [d] Residual weight % at 800 °C in nitrogen.

of the baseline shift; all PIs had high T_g (>276 °C). The lowest T_g value (276 °C, measured by DSC) belongs to **5c**, which has the flexible ether groups of ODPA moiety, and the highest T_g values are obtained for **5f**, which contains the more rigid NTDA unit. Unexpectedly, the T_g values of **5** series were about 11−16 °C higher than that of the corresponding **6** series derived from the symmetric diamine. Molecular symmetry allows better packing, and stronger interchain interactions, which should enhance the T_g value. However, **6** series with symmetric structure had relatively low T_g. The increased T_g values of **5** series is ascribed to a restriction of molecular mobility (i.e., the neighboring benzene ring) caused by the di-*tert*-butyl groups, which did not allow an easy chains rotating. In other words, the incorporation of the asymmetric di-*tert*-butyl pendent groups into the polymer chain significantly enhances the rotational barrier of the polymer chains and thus increases the T_g of **5** series. The NMR results of monomers suggest that the neighboring benzene ring is prohibited from free rotation by the steric hindrance of the bulky di-*tert*-butyl groups. More detailed information can be obtained from the dynamic mechanical behavior measurements take of the films as a function of temperature. Herein, films of around 60 μm thickness were studied between 0 and 400 °C. The mechanical relaxation spectra of **5a** are shown in Figure 6. On the basis of tan δ and E'' peaks, a glass transition was observed at 375 °C. Such a transition is associated with an ∼2 orders of magnitude decrease in E'. The mechanical relaxation spectra of the other PIs **5** series resemble those of **5a**. Table 4 also summarizes the glass transition temperatures of **5** series. Polymers **5** series exhibited high glass transition temperatures of 310−398 °C. The higher T_gs, i.e., **5f**, are attributed to the fact that the rotations of these bonds are hindered by the rigid structures within the NTDA dianhydride moiety of the PIs, causing chain stiffness to increase. It is noteworthy that the soluble PIs **5a** and **5f** have very high T_gs (i.e., 375 and 398 °C). The high-T_g materials are important for high-temperature application.

Table 2. Solubility of Polyimides[a]

polymer	NMP	DMAc	*o*-chlorophenol	$CHCl_3$	THF	cyclohexanone	acetone
5a	++	++	++	++	++	++	−
5b	++	++	++	++	++	++	−
5c	++	++	++	++	++	++	−
5d	++	++	++	++	++	++	++
5e	++	++	++	++	++	+	−
5f	+	+−	++	++	+−	+−	−
6c	−	−	+−	−	−	−	−
6e	−	−	−	−	−	−	−

[a] Solubility: ++, soluble at room temperatures; +, soluble on heating at 60 °C; +−, partial soluble in heating at 60 °C, unsoluble. Abbreviations: NMP, *N*-methyl-2-pyrrolidone; DMAc, *N,N*-dimethylacetamide; THF, tetrahydrofuran.

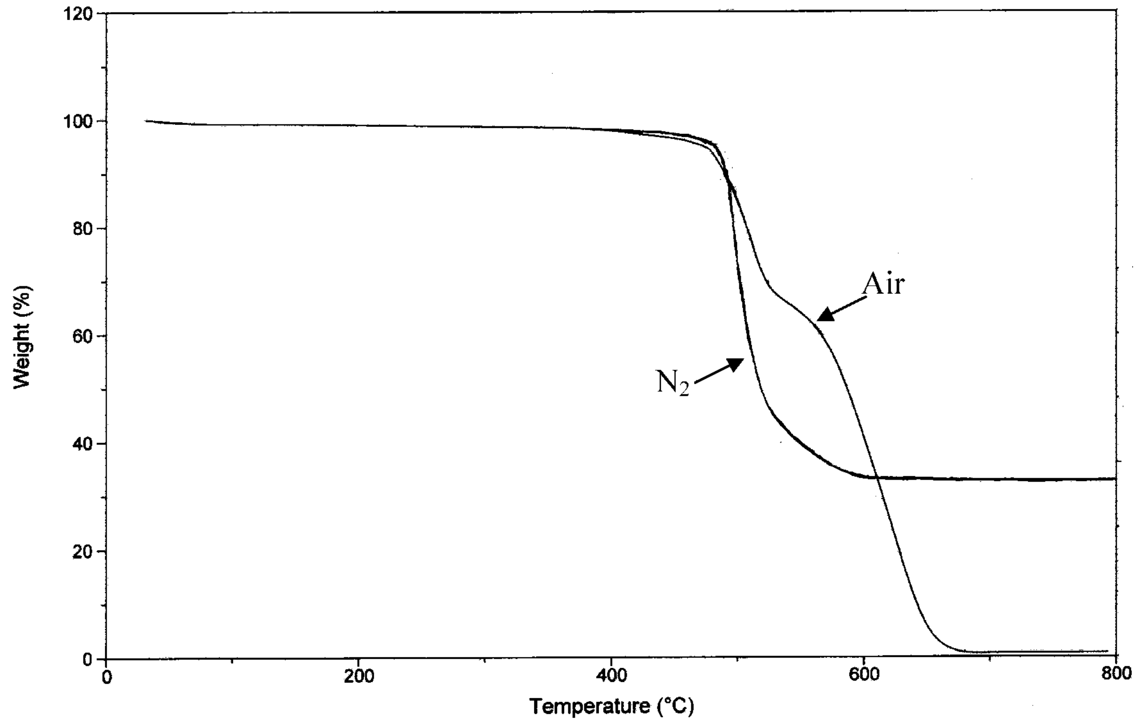

Figure 5. TGA thermograms of polyimides **5e** at a scan rate of 10 °C/min.

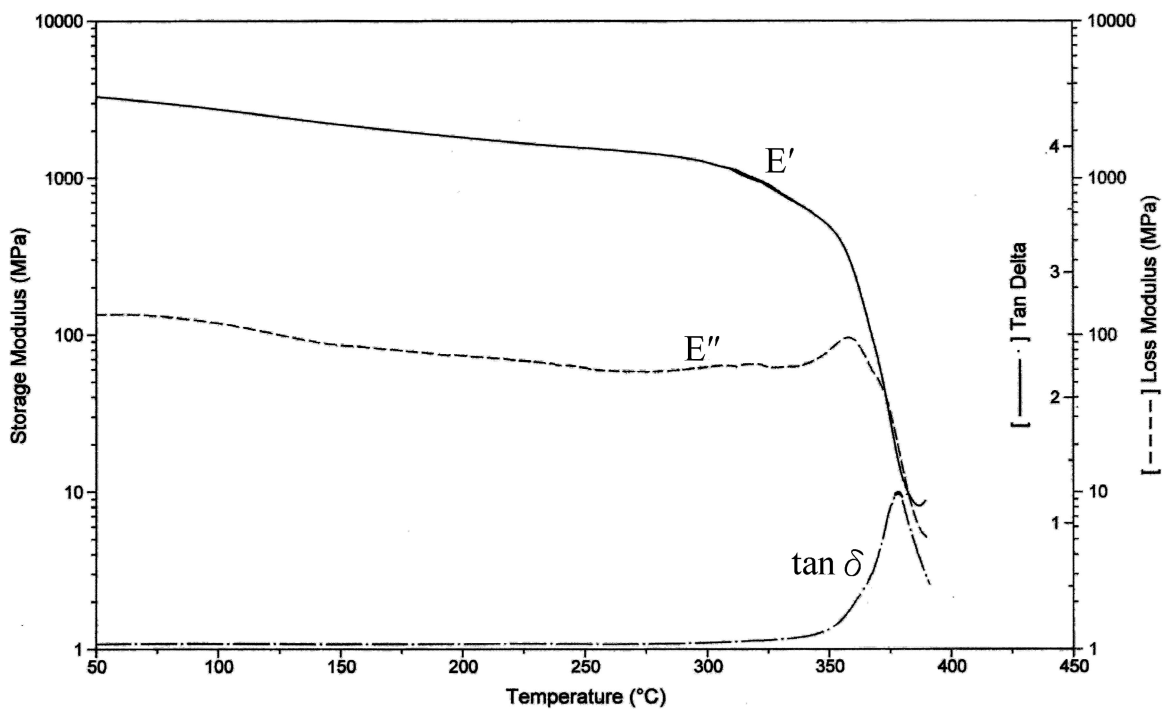

Figure 6. Dynamic mechanical analysis curves for **5a** at a heating rate of 5 °C/min.

Conclusions

Incorporation of the bulky *tert*-butyl groups can impart a decrease in PI density due to decreased packing. Introduction of the asymmetric *tert*-butyl groups leads to the formation of configuration isomers of the repeat unit along the polymer backbone and causes the decrease in the intermolecular force and packing ability of the resulting polymers. Thus, PIs **5** series containing the asymmetric *tert*-butyl groups exhibited excellent solubility and low dielectric constant (i.e., 2.74−2.92). For example, **5a** derived from rigid PMDA was soluble in NMP, DMAc, *o*-chlorophenol, chloroform, THF, and cyclohexanone. Unexpectedly, the T_g values of **5** series were about 11−16 °C higher than that of the corresponding **6** derived from the symmetric diamine. The increased T_g values of **5** series is ascribed to a restriction of molecular mobility (i.e., the neighboring benzene ring) caused by the di-*tert*-butyl groups. The soluble **5a** and **5g** derived from the rigid PMDA and NTDA had high T_g, which were 375 and 398 °C, respectively (measured by DMA). The crystal structure of compound **8** indicates that the symmetric compound leads to the strong intermolecular interaction and good packing ability.

Acknowledgment. We appreciate the financial support provided by the National Science Council through Project NSC.

References and Notes

(1) Hougham, G.; Tesoro, G.; Shaw, J. *Macromolecules* **1994**, *27*, 3642.
(2) Feiring, A. E.; Auman, B. C.; Wonchoba, E. R. *Macromolecules* **1993**, *26*, 2779.
(3) Irvin, J. A.; Neef, C. J.; Kane, K. M.; Cassidy, P. E.; Tullos, G.; St. Clair, A. K. *J. Polym. Sci., Part A: Polym. Chem.* **1992**, *30*, 1675.
(4) Long, T. M.; Swager, T. M. *J. Am. Chem. Soc.* **2003**, *125*, 14113.
(5) Tsuchiya, K.; Ishii, H.; Shibasaki, Y.; Ando, S.; Ueda, M. *Macromolecules* **2004**, *37*, 4794.
(6) Hrubesh, L. W.; Keene, L. E.; Latorre, V. R. *J. Mater. Res.* **1993**, *8*, 1736.
(7) Wu, S.; Hayakawa, T.; Kikuchi, R.; Grunzinger, S. J.; Kakimoto, M.-A. *Macromolecules* **2007**, *40*, 5698.
(8) *Polyimide: Fundamental and Applications*; Ghosh, M. M., Mittal, K. L., Eds.; Marcel Dekker: New York, 1996.
(9) Eastmond, G. C.; Paprotny, J. *Macromolecules* **1995**, *28*, 2140.
(10) Imai, Y. *High Perform. Polym.* **1995**, *7*, 337.
(11) Eastmond, G. C.; Gibas, M.; Paprotny, J. *Eur. Polym. J.* **1999**, *35*, 2097.
(12) Chern, Y. T.; Shiue, H. C. *Macromolecules* **1997**, *30*, 4646.
(13) Mathias, L. J.; Muir, A.V. G.; Reichert, V. R. *Macromolecules* **1991**, *24*, 5232.
(14) Matsuura, T.; Hasuda, Y.; Nishi, S.; Yamada, N. *Macromolecules* **1991**, *24*, 5001.
(15) Li, F.; Fang, S.; Ge, J. J.; Honigfort, P. S.; Chen, J. C.; Harris, F. W.; Cheng, S. Z. D. *Polymer* **1999**, *40*, 4571.
(16) Li, F.; Fang, S.; Ge, J. J.; Honigfort, P. S.; Chen, J. C.; Harris, F. W.; Cheng, S. Z. D. *Polymer* **1999**, *40*, 4987.
(17) Hsiao, S. H.; Yang, C. P.; Yang, C. Y. *J. Polym. Sci., Part A: Polym. Chem.* **1997**, *35*, 1487.
(18) Reddy, D. S.; Shu, C. F.; Wu, F. I. *J. Polym. Sci., Part A: Polym. Chem.* **2002**, *40*, 3615.
(19) Yagci, H.; Mathias, L. J. *Polymer* **1998**, *39*, 3779.
(20) Yang, C. P.; Su, Y. Y.; Wu, K. L. *J. Polym. Sci., Part A: Polym. Chem.* **2004**, *42*, 5424.
(21) Chung, I. S.; Kim, S. Y. *Macromolecules* **2000**, *33*, 3190.
(22) Liaw, D. J.; Liaw, B. Y. *J. Polym. Sci., Part A: Polym. Chem.* **1997**, *35*, 1527.
(23) Zheng, H. B.; Wang, Z. Y. *Macromolecules* **2000**, *33*, 4310.
(24) Gao, C. L.; Wu, X. E.; Lv, G. H.; Ding, M. X.; Gao, L. X. *Macromolecules* **2004**, *37*, 2754.
(25) Li, J.; Kato, J.; Kudo, K.; Shiraishi, S. *Macromol. Chem. Phys.* **2000**, *201*, 2289.

MA802305Q